in Proceedings off
ADVANCED MEMS FOR RF AND MILLIMETER
WAVE COMMUNICATIONS

EDITURA ACADEMIEI ROMANE
Bucuresti, 2005

Reliability Aspects of Thermal RF-Sensing Structures on Micromachined AlGaAs/GaAs Membranes

K. MUTAMBA[1], C. SYDLO[1], L. DIVAC KRNIC[2], B. MOTTET[1], I. AHMED ALI[3], H. L. HARTNAGEL[1]

[1]Institut fuer Hochfrequenztechnik, TU Darmstadt, Merckstr. 25, 64283 Darmstadt, Germany.
E-mail: mutamba@hf.tu-darmstadt.de

[2]Multimedia Communications Lab, TU Darmstadt, Merckstr. 25, 64283 Darmstadt, Germany.

[3]King Faisal University, P O Box 420, Al-Ahsa 31982, Kingdom of Saudi Arabia.

Abstract. This paper reports on a reliability analysis made on micromachined millimeter-wave power sensing structures by means of electrical pulses. As the main result of the pulsed electrical stress a degradation of the sensor bolometric termination is observed. Different geometries are considered and the corresponding degradation process analysed.

1. Introduction

Electromechanical and thermal-electrical mechanisms are the most used sensing and actuation schemes in micromachined devices. While they are mainly used to produce deflection of microbeams, cantilevers and membranes for actuation functions, they play a key role in sensors to provide sensitive transduction mechanisms [1]. An example of the latter is the widely known principle of thermal isolation in micromachined bolometric sensors for gas flow and microwave power measurement (Fig. 1(a)). Here thin membranes with defined geometry and boundary conditions help to realise small areas of defined thermal conductivity to the rest of the chip, allowing to reach high temperature gradients. For the GaAs-based technology an Aluminium mole-content of 48% in the AlGaAs membrane provides the maximal thermal resistance. The relatively strong thermoelectric properties of GaAs are used to form the thermocouple measuring

the generated temperature difference. This can result from rf power losses in a dedicated transmission line or from the absorbed power in a matched termination [2], [3]. The reached sensitivities as well as the compatibility of the fabrication process with MMIC technologies make them suitable for the integration of power detection and monitoring functions in microwave ICs.

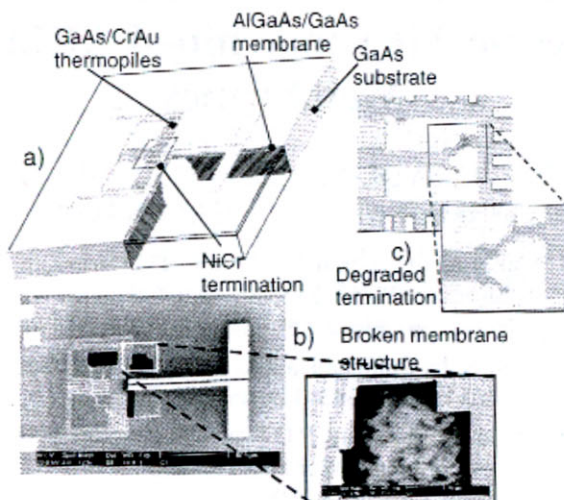

Fig. 1. Schematics of the investigated power sensor device a), here with a receiving dipole antenna for 60 GHz. Failure modes related to mechanical b) and electrical c) reliability are shown.

To ensure a commercial viability to the developed devices requires thorough reliability investigations. While from the mechanical point of view the fragility of the thin 1 to 2 micron membrane is the main issue, limitation to power handling capabilities can arise from the stability of the used metallisation system for the definition of transmission lines and termination (Fig. 1 b) and c)). Here tradeoffs are needed as, for example, to the question of using thicker membranes which are mechanically stable and provide a reduced sensitivity.

The reliability investigation of this work uses the transmission-line pulse (TLP) method to analyse failure and degradation mechanisms of thermal power sensing structures. It includes a first analysis on an integrated 60 GHz bolometer with a NiCr termination on the membrane and GaAs/CrAu thermopiles for the dc output. This is followed by a more systematic study of termination structures with different geometries. The main degradation mechanism has been identified to be a current induced metal migration at regions of high current densities followed by a field induced material transport in the damaged regions. Subsequent material analysis support this description.

2. Experiment Description and Discussion

a) Temperature distribution

Preliminary investigations have been made to determine the temperature distribution due to a dc current flow in a termination. The NiCr(80/20) termination is here located on the top side of the 150 microns thick bulk sensor before the backside process to selectively etch the membrane. To determine the resulting distribution a liquid crystal (LC) thermography has been made with a coating of 0.7°C bandwidth between 35 and 35.7°C (R35C0.7W). The temperature distribution of Fig. 2 has been obtained for a power level of 150 mW. Comparable results, shown in Fig. 3, have also been obtained from a thermal FEM calculation with the ANSYS software. These results show that besides the requirement for the hot ends of the thermocouples to be in the closest neighbourhood of the heating resistor for higher sensitivities, the contours of the temperature distribution can be used to define an optimal arrangement of the thermocouples.

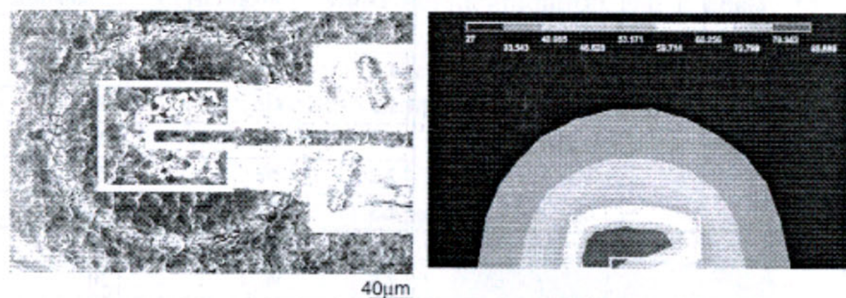

Fig. 2. Measured and calculated temperature distribution around the NiCr heating resistor on the substrate. The obtained profile corresponds to an electrical dc power level of 150 mW in the resistor. The R35C0.7W LC-coating was used.

b) TLP Measurement set up

The used TLP reliability system is computer-controlled and mainly consists of a parameter analyser (HP4145A), a pulse generator (HP8114A), an oscilloscope (TDS620) for pulse response monitoring and a switching matrix. Additional probe-heads have been designed and realised for this purpose. A microscope camera takes a picture after each stress cycle. All components are computer-controlled and allow a fully automated testing procedure. A dedicated software has been written to provide high flexibility in stress and measurement cycles. This set-up allows device-specific stress and analysis procedures for the identification of degradation mechanisms with any metallization. The short pulse of the TLP method is

generally shorter than the thermal time constant of the sensor. This allows for higher amplitudes of the DC input signal with minimum device heating and well-defined electrical stress. Furthermore, a time-domain analysis of the data is possible, allowing for precise calculation of thermal and electrical models [4], [5].

c) Detection of degradation threshold

The threshold detection measurement is performed on resistors of different geometry as described in Fig. 3 and the table, using electrical pulses with a length of 100 ns. The influence of the chosen geometry on the device power handling capabilities is determined by varying the amplitude of the pulses applied to the device under test. Degradation is detected by the subsequent IV-measurements of the devices after a stress cycle. A rise in resistivity is observed when degradation occurs. Below the respective threshold voltages, no change of the resistance could be observed, even with an increase of the pulse numbers.

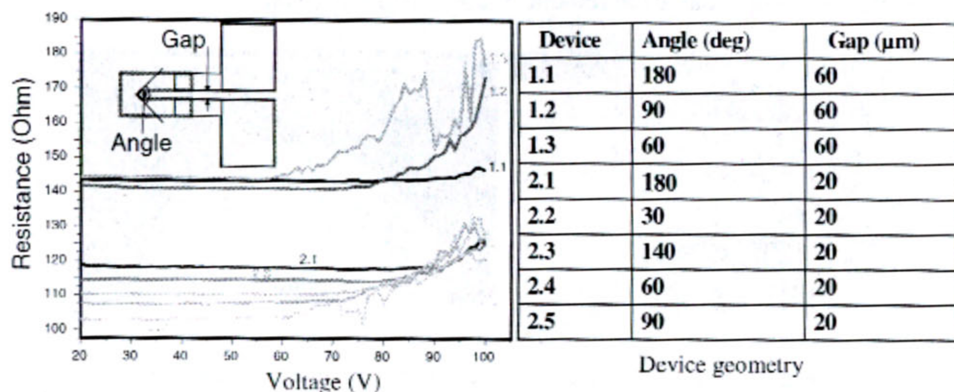

Device	Angle (deg)	Gap (µm)
1.1	180	60
1.2	90	60
1.3	60	60
2.1	180	20
2.2	30	20
2.3	140	20
2.4	60	20
2.5	90	20

Device geometry

Fig. 3. Change of resistance as a function of the applied electrical stress. Relevant geometric parameters and the corresponding values are respectively indicated in the inset and the table. Structures with sharp included angles show a lower degradation threshold.

As shown in the measurement results in Fig. 3, a lower degradation threshold is observed on the samples with lower included angle. This threshold reduction can be explained by the current density increase in the corner region.

d) Failure mechanism investigations

The main device failure mechanism has been identified to be the degradation of the NiCr termination resistor with increasing input power.

Initially, the degradation occurs in the regions with the highest current density (Figs. 4a, 2–4) and therefore highest thermal excitation. The electrons drift towards the anode leaving positively charged ion cores to be influenced by two types of forces. The electrostatic force attracts the ions towards the cathode and the momentum exchange between electrons and ion cores makes them migrate towards the anode. This leads to a current induced metal migration of the NiCr resistor metal and a damage to the unpassivated underlying GaAs surface.

The observed material transport is facilitated by the combined effect of local high temperatures and high current densities. With progressing degradation the resistance locally increases and therefore leads to high electric fields in the already damaged regions (Figs. 4a., 5–9). As a result, a second material transport mechanism is observed, which includes now also the GaAs surface. Sub-picture 8 and 9 in Fig. 4 show small particles close to the burned areas indicating a transport of material away from the damaged regions of the NiCr resistor.

This description of the degradation process is also supported by a material analyse based on energy dispersive x-ray (EDX), as shown in Fig. 4b. This technique was used immediately after degradation and it allows to show the composition of the transported material, which includes mainly GaAs from the substrate and a lower amount of the used metallization materials as shown in figure 4. The relatively high Cr content compared to Ni is due to presence of Cr as an adhesion layer for Au metallisation.

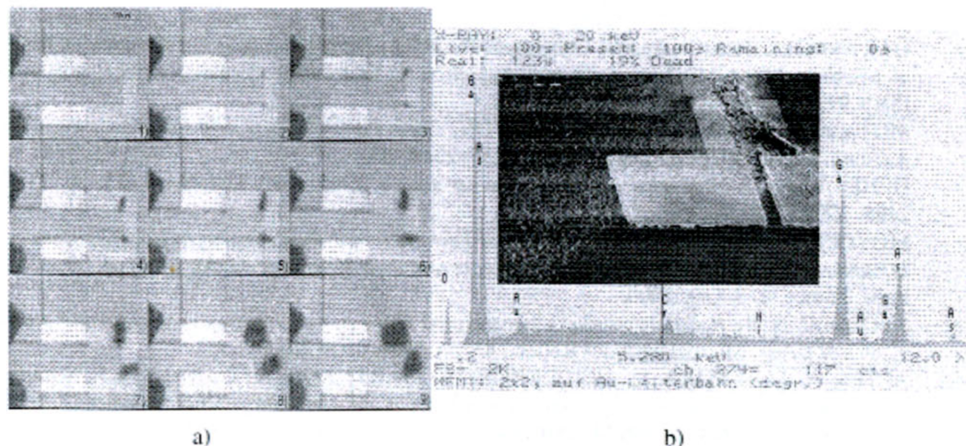

a) b)

Fig. 4. a) Degradation process in the NiCr test resistor. Current induced effects as appearing in subpictures 2–4 are followed by field induced effects from subpicture 5 on (device 1.1). b) Energy dispersive x-ray analysis of the material transport in a degraded structure before cleaning (device 2.5). The inset shows the removal of material below the metallisation.

3. Conclusion

The pulsed approach for the excitation of degradation mechanisms has been used to study the reliability of a power sensor structure. The main advantage of the degradation analysis is the possibility to stop the degradation process at any stage for sufficient measurements and analysis. This work shows the importance of the chosen approach for the improvement of sensor design and technology. For this type of resistance structures the current induced degradation mechanisms trigger the field induced ones by producing a pre-damage into the structure of the underlying substrate material. Without such a pre-damage a pure field induced degradation is not observed. Additional measurements and simulations are needed for an optimal sensor design. These can include methods such as the 3 ω technique for the determination of thermal transport properties of thin multilayer structures [6]. Coupled fields analysis are also needed for a complete design including a maximum of the involved physical effects and reliable material data.

Acknowledgements. We would like to thank Mr. Mike Norman of Hallcrest Ltd, Poole, UK for providing the LC coating. The work of Dr. Ahmed Idris Ali was supported by the German Academic Exchange Service (DAAD).

References

[1] HARTNAGEL, H.L. et al., *III-V compound MEMS and optical communication tunable filters*, in Micromachined Microwave devices and circuits, Editura Academici Romane, pp.10–23, ISBN 973-27-0908-1, 2002.

[2] MUTAMBA, K. et al., *Micromachined 60 GHz GaAs Power Sensor with Integrated Receiving Antenna*, Digest IEEE MTT-S 2001, pp. 2235–2238, 2001.

[3] DEHÉ, A., et al., *Integrated microwave power sensor*, Electronics Letters, 31, 25, pp. 2187–2188, 1995.

[4] MOTTET, B., et al., *Pulsed Electrical Stress Techniques for the detection of Non-Thermal Lifetime-Problems with Semiconductor Devices and their IC's*, Proc. GaAs 2000, pp. 39–43, Paris, France, 2.-3. Oct. 2000.

[5] SYDLO, C. et al., *Reliability sudies on integrated GaAs power-sensor structures using pulsed electrical stress*, Microelectronics Reliab., **43**, pp. 1929–1933, 2003.

[6] ALTES, A., MUTAMBA, K., HEIDERHOFF, R., HARTNAGEL, H.L., BALK, L.J., *Scanning near-field thermal conductivity measurements on a micromachined thin membrane*, to be published in Superlattices and Microstructures.